Doppler Effect Reduction in an OFDM System Thanks to Massive MIMO

Alexis Bazin, Bruno Jahan, Maryline Hélard

IEEE Access
Multidisciplinary | Rapid Review | Open Access Journal

Received May 18, 2018, accepted July 3, 2018, date of publication July 9, 2018, date of current version July 30, 2018.

Digital Object Identifier 10.1109/ACCESS.2018.2854001

Doppler Effect Reduction in an OFDM System Thanks to Massive MIMO

ALEXIS BAZIN[1], (Student Member, IEEE), BRUNO JAHAN[1], AND MARYLINE HÉLARD[2], (Member, IEEE)

[1]Department of Advanced Wireless Evolution, Orange Labs, 35512 Cesson-Sévigné, France
[2]INSA Rennes, CNRS, Institut d'Electronique et de Télécommunications de Rennes, University of Rennes 1, 35700 Rennes, France

Corresponding author: Alexis Bazin (alexis.bazin@orange.com)

ABSTRACT Among many challenges, 5G should improve the quality of service for moving users. In such a mobility context, the Doppler effect creates interference which can severely damage the performance of the systems. The effect of very large number of uncorrelated receive antennas on the Doppler effect is studied in this paper with a simple maximum ratio combining receiver and the orthogonal frequency division multiplexing modulation. This paper relies on an analytical analysis of the signal-to-interference ratio (SIR) and on a statistical analysis of the propagation channel. Therefore, the contribution of this paper is twofold. First, the asymptotic SIR is analytically expressed when the number of receive antennas tends toward infinity. Second, the decrease of the impact of the Doppler effect with the increase of the number of receive antennas is demonstrated, proving that a massive multiple-input multiple-output system with a low-complexity maximum ratio combining receiver can be used to improve the quality of service in mobility scenarios. Finally, the simulation results highlight the impact of such a massive multiple-input multiple-output system in practice.

INDEX TERMS 5G, Doppler effect, massive MIMO, OFDM.

I. INTRODUCTION

The global increase of the mobile data consumption as well as the multiplication and diversification of the connected devices push the development of the Fifth Generation of cellular networks (5G) [1]. Many studies foresee the emergence of new use cases with mobility such as Vehicle-To-Vehicle (V2V) or, more generally, Vehicle-To-everything (V2x) communications [2], [3]. In those scenarios and according to [4], the speed of the users can be as high as 500 km/h. Thus, when using a multi-carrier modulation such as the Orthogonal Frequency Division Multiplexing (OFDM) modulation, the Inter-Carrier Interference (ICI) due to the Doppler effect might have a detrimental impact on the performance of the systems [5]. Therefore, solutions are investigated to counteract this effect, stabilizing the high mobility communications.

With the existing Doppler effect reduction schemes, good performance comes with an increased complexity [6], [7]. Additionally, the use of multiple antennas in a Multiple-Input Multiple-Output (MIMO) system can be exploited to mitigate the interference due to the mobility. For example, in a Line-Of-Sight (LOS) environment the creation of a beam towards the transmitter using a directional antenna [8], [9] or several antennas reduces the angular spread and thereby limits the Doppler effect. This property has been exploited in [10] and [11] for flat fading channels. Moreover, ICI compensation techniques for MIMO-OFDM systems can take advantage of the diversity on the transmitter side [12], on the receiver side [13], [14] or both on the transmitter side and on the receiver side [15], [16].

A large increase of the number of antennas is commonly called massive MIMO and is a popular trend for the development of 5G [17]. Using the large diversity offered by massive MIMO systems, the performance can be greatly improved even with low-complexity transmitters and receivers. When these numerous antennas are used on the transmitter side, the transmitted signal can be focused towards the receivers, the received power is enhanced, the multiuser interference is reduced and thereby multiuser communications are allowed based on the so-called Spatial Division Multiple Access (SDMA) techniques [18]. This paper focuses on a massive MIMO system where the numerous number of antennas are located on the receiver side and the transmitter is equipped with a single antenna. Therefore, the Signal-to-Interference-plus-Noise Ratio (SINR) is increased on the

receiver side by reducing the noise power and the multiuser interference power as highlighted in [19]–[22]. Accordingly, one may wonder if a massive MIMO system with a simple receiver could efficiently reduce the ICI.

Unlike [10] and [11], this paper focuses on the challenging problem of Doppler effect reduction for Non-Line-Of-Sight (NLOS) OFDM communications, where the received signals arrive from all directions with equal probability [23]–[25]. This situation happens frequently in an urban environment. While the previous studies take into account a small number of antennas on the receiver side (2 in [13] and [14] and up to 5 in [15] and [16]), the effect of a very large number of uncorrelated receive antennas on the ICI is analytically studied considering a low-complexity Maximum Ratio Combining (MRC) receiver. In this context, this study analytically highlights two aspects:

- the impact of an increase of the number of receive antennas,
- the asymptotic behavior, when the number of receive antennas tends towards infinity.

Moreover, simulation results confirm the analytical results and highlight the impact of the proposed massive MIMO system in practice. This paper can be used as a basis for further studies on massive MIMO systems in high mobility scenarios.

Firstly, the system model is presented in section II in order to highlight the interference due to the Doppler effect in the considered system. Then, the Signal-to-Interference Ratio (SIR) of the system is analyzed in part III, as this metric allows for linking the impact of the Doppler effect and the number of receive antennas. This analysis leads to an expression of the asymptotic SIR, when the number of receive antennas tends towards infinity. Moreover, a necessary and sufficient condition is proposed to show how an increase of the SIR is related to an increase of the number of receive antennas. However, both results rely on the statistical properties of the propagation channel. With the statistical analysis of the channel components in part IV, this problem is solved and the asymptotic SIR as well as the necessary and sufficient condition can be analytically expressed. Finally, the simulation results are given in part V in terms of SIR and of Bit Error Rate (BER) and help to draw a conclusion in the last section.

The following notations are used in this paper. For a complex scalar, $|\,.\,|$ denotes the norm and $(\,.\,)^*$ the complex conjugate. Moreover, $E[\,.\,]$ stands for the expected value and $\mathcal{F}[\,.\,]$ for the Fourier transform operator. Vectors and matrices are represented in boldface letters and $(\,.\,)^T$ represents their transpose, $(\,.\,)^H$ their conjugate transpose and $\|\,.\,\|$ their Euclidean norm.

II. SYSTEM MODEL

In order to evaluate the impact of the Doppler effect on massive MIMO systems, an uplink transmission between a moving user equipped with a single antenna and a Base Station (BS) equipped with N_r antennas is considered in this paper. It can be noted that this scenario can be extended to a V2V scenario considering a moving receiver instead of a BS. Regarding the reduced coherence time, channel estimation and equalization processes are both conducted on the BS side during the same time slot. Therefore, the proposed scheme for uplink can be applied with Frequency Division Duplex (FDD) or Time Division Duplex (TDD) modes. Fig. 1 depicts the considered scenario. Thereafter, the system model is described and the SIR is deduced in order to have a metric bringing together the impact of the Doppler effect and the number of receive antennas N_r.

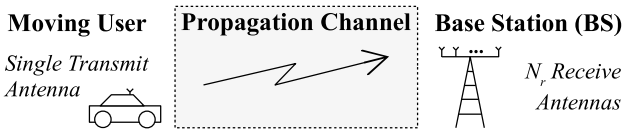

FIGURE 1. Considered scenario: an uplink transmission between a moving user equipped with a single antenna and a BS equipped with N_r antennas.

On the transmitter side, an OFDM modulation is used with a FFT size denoted by M and an inter-carrier spacing indicated by F_0. According to [26], the baseband signal in the time domain of an OFDM symbol can be defined by:

$$s(t) = \sum_{m=0}^{M-1} c[m] e^{j2\pi m F_0 t}, \tag{1}$$

$c[m]$ being the complex data on sub-carrier m. A long enough Cyclic Prefix (CP) is added before this symbol in order to avoid Inter-Symbol Interference (ISI).

In general, the propagation channel can be divided in two components: a LOS component and a NLOS component [27], as in [28] and [29] for example. On the one side, for the LOS component the Doppler effect translates into a Doppler shift for which compensation techniques have been widely studied in the literature, for example in [30] and [31]. On the other side, for the NLOS component the Doppler effect translates into a Doppler spread. In this paper, a NLOS communication with Doppler spread is considered and the propagation channel is modeled by a multi-path Rayleigh fading channel model with L_h independent paths. As the user is moving, each path varies over time because of the Doppler spread and according to the Jakes' Doppler spectrum [24]. The variations over time of the l^{th} multi-path component between the transmitter and the receive antenna n_r are given by $h_l^{n_r}(t)$ while the time delay of the l^{th} multi-path component is denoted by τ_l. Moreover, the receive antennas are sufficiently spaced so that $h_l^{n_r}(t)$ and $h_l^{n_r'}(t)$ can be assumed as independent variables if $n_r \neq n_r'$. The received signal on the antenna n_r is expressed in the time domain by $r^{n_r}(t)$ and is defined as follows:

$$r^{n_r}(t) = \sum_{l=0}^{L_h-1} s(t-\tau_l) h_l^{n_r}(t) + \eta^{n_r}(t), \tag{2}$$

with $\eta^{n_r}(t)$ the time domain noise component on the antenna n_r. Focusing on a particular sub-carrier m_0, the notation $c_p = c[m_0 - p]$ is given and the mathematical sets of integer Ω_p and Ω_p^* are defined as follows:

$$\Omega_p = \{p \in \mathbb{Z} \mid c_p \neq 0\}, \tag{3}$$

being the set of useful sub-carriers and:

$$\Omega_p^* = \Omega_p \setminus \{0\}, \tag{4}$$

being the set of useful sub-carriers without the sub-carrier index m_0. Therefore, as the CP avoids the ISI and using (1) in (2), $r^{n_r}(t)$ becomes:

$$r^{n_r}(t) = \sum_{p\in\Omega_p} c_p \sum_{l=0}^{L_h-1} h_l^{n_r}(t) e^{j2\pi(m_0-p)F_0(t-\tau_l)} + \eta^{n_r}(t). \tag{5}$$

After the demodulation process, the received data on sub-carrier m_0 and on the antenna n_r is:

$$\begin{aligned} y^{n_r} &= F_0 \left(\int_0^{1/F_0} r^{n_r}(t) e^{-j2\pi m_0 F_0 t} dt \right) \\ &= \sum_{p\in\Omega_p} c_p \sum_{l=0}^{L_h-1} F_0 \times \left(\int_0^{1/F_0} h_l^{n_r}(t) e^{-j2\pi p F_0 t} dt \right) \\ &\quad \times e^{-j2\pi(m_0-p)F_0\tau_l} + F_0 \left(\int_0^{1/F_0} \eta^{n_r}(t) e^{-j2\pi m_0 F_0 t} dt \right) \end{aligned} \tag{6}$$

or equivalently:

$$y^{n_r} = \sum_{p\in\Omega_p} H_p^{n_r} c_p + b^{n_r}, \tag{7}$$

with:

$$b^{n_r} = F_0 \left(\int_0^{1/F_0} \eta^{n_r}(t) e^{-j2\pi m_0 F_0 t} dt \right), \tag{8}$$

being the noise component on the antenna n_r and:

$$H_p^{n_r} = \sum_{l=0}^{L_h-1} F_0 \left(\int_0^{1/F_0} h_l^{n_r}(t) e^{-j2\pi p F_0 t} dt \right) e^{-j2\pi(m_0-p)F_0\tau_l}. \tag{9}$$

For the link between the user and the antenna of index n_r at the BS, $H_0^{n_r}$ represents the component of the channel that allows for receiving the useful data c_0. On the contrary, $H_{p\in\Omega_p^*}^{n_r}$ are the components of the channel that lead to ICI on the data c_0 carried out by the adjacent sub-carriers $c_{p\in\Omega_p^*}$. Thus, if the propagation channel is static, $H_{p\in\Omega_p^*}^{n_r} = 0$. With N_r receive antennas, the following channel vectors are defined:

$$\mathbf{H}_p^{(N_r)} = \left[H_p^0 \quad H_p^1 \quad \cdots \quad H_p^{N_r-1} \right]^T, \tag{10}$$

with $p \in \Omega_p$, the noise vector is:

$$\mathbf{b}^{(N_r)} = \left[b^0 \quad b^1 \quad \cdots \quad b^{N_r-1} \right]^T, \tag{11}$$

and the received data vector before equalization is given by:

$$\mathbf{y}^{(N_r)} = \left[y^0 \quad y^1 \quad \cdots \quad y^{N_r-1} \right]^T. \tag{12}$$

The propagation channel is estimated via pilots on the BS side. A perfect channel estimation is assumed for the sake of simplicity and the receiver performs an equalization using the low-complexity MRC technique. Thus, after the MRC processing, the received data $\hat{c}_0$ is:

$$\begin{aligned} \hat{c}_0 &= \frac{\left(\mathbf{H}_0^{(N_r)}\right)^H}{\left\|\mathbf{H}_0^{(N_r)}\right\|^2} \mathbf{y}^{(N_r)} \\ &= c_0 + \underbrace{\sum_{p\in\Omega_p^*} \frac{\left(\mathbf{H}_0^{(N_r)}\right)^H \mathbf{H}_p^{(N_r)}}{\left\|\mathbf{H}_0^{(N_r)}\right\|^2} c_p}_{I_{Doppler}} + \underbrace{\frac{\left(\mathbf{H}_0^{(N_r)}\right)^H \mathbf{b}^{(N_r)}}{\left\|\mathbf{H}_0^{(N_r)}\right\|^2}}_{b_{Noise}}. \end{aligned} \tag{13}$$

The received data $\hat{c}_0$ is thus affected by the ICI due to the Doppler effect $I_{Doppler}$ and by the noise component b_{Noise}.

The system model as well as the notations are summarized by Fig. 2, which highlights the ICI created by the Doppler effect.

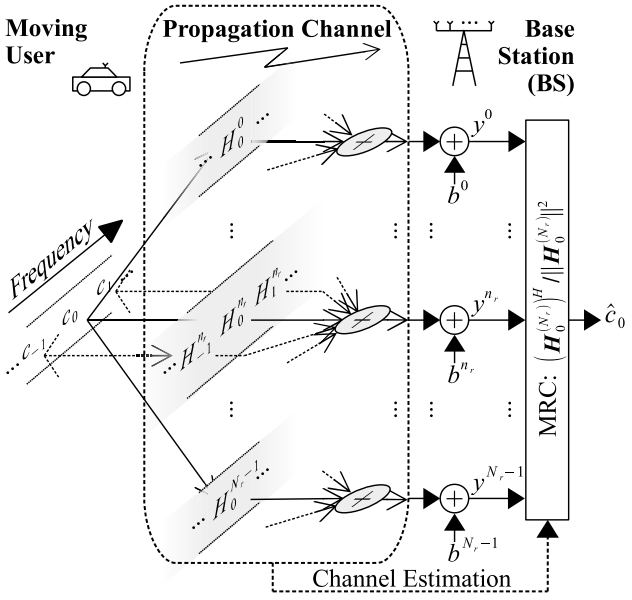

FIGURE 2. System model for an uplink transmission between a single-antenna moving user and a BS with N_r antennas.

III. SIR ANALYSIS

The aim of this part is to analytically evaluate the impact of the ICI created by the Doppler effect as highlighted in equation (13). One can see that the noise component b_{Noise} in (13) is not impacted by the Doppler effect. Therefore, this

noise component is not taken into account in this analytical study for the sake of clarity. In order to evaluate only the impact of the Doppler effect, the SIR is a relevant metric as the ICI component $I_{Doppler}$ is the only interference affecting the received data. Firstly, the SIR with N_r receive antennas $\gamma^{(N_r)}$ is expressed in part III-A using the system model of the previous part. Then, the asymptotic value of this SIR when $N_r \to +\infty$ is expressed in part III-B. Finally, in part III-C a comparison between $\gamma^{(N_r)}$ and $\gamma^{(N_r+1)}$ provides a necessary and sufficient condition to have an increase of the SIR when increasing N_r.

A. EXPRESSION OF THE SIR

From the equation (13), the SIR $\gamma^{(N_r)}$ with N_r receive antennas can be deduced:

$$\gamma^{(N_r)} = \frac{\left\|\mathbf{H}_0^{(N_r)}\right\|^4}{\sum_{p\in\Omega_p^*}\left|\left(\mathbf{H}_0^{(N_r)}\right)^H \mathbf{H}_p^{(N_r)}\right|^2} = \frac{\left(\sum_{n_r=0}^{N_r-1}\left|H_0^{n_r}\right|^2\right)^2}{\sum_{p\in\Omega_p^*}\left|\sum_{n_r=0}^{N_r-1}\left(H_0^{n_r}\right)^* H_p^{n_r}\right|^2}. \quad (14)$$

Since the only interference taken into account is due to the Doppler effect, an increase of the SIR $\gamma^{(N_r)}$ is equivalent to a decrease of the impact of the Doppler effect. Obviously, the number of receive antennas N_r has an impact on $\gamma^{(N_r)}$ as it gives the size of the channel vectors $\mathbf{H}_p^{(N_r)}$ with $p \in \Omega_p$.

B. ASYMPTOTIC SIR

Owing to the law of large numbers, when the number of receive antennas N_r tends towards infinity ($N_r \to +\infty$), the denominator of (14) becomes:

$$\begin{aligned}\sum_{p\in\Omega_p^*}\left|\left(\mathbf{H}_0^{(N_r\to+\infty)}\right)^H \mathbf{H}_p^{(N_r\to+\infty)}\right|^2 &= \sum_{p\in\Omega_p^*}\left|N_r E\left[\left(H_0^{n_r}\right)^* H_p^{n_r}\right]\right|^2 \\ &= N_r^2 \sum_{p\in\Omega_p^*}\left|E\left[\left(H_0^{n_r}\right)^* H_p^{n_r}\right]\right|^2, \quad (15)\end{aligned}$$

and the numerator of (14) becomes:

$$\left\|\mathbf{H}_0^{(N_r\to+\infty)}\right\|^4 = N_r^2 E\left[\left|H_0^{n_r}\right|^2\right]^2. \quad (16)$$

Thereby, using (15) and (16) in (14), the asymptotic SIR is defined by:

$$\gamma_\infty = \frac{\left(E_0^{(1)}\right)^2}{\sum_{p\in\Omega_p^*}\left|E_p^{(1)}\right|^2}, \quad (17)$$

with:

$$E_p^{(1)} = E\left[\left(H_0^{n_r}\right)^* H_p^{n_r}\right]. \quad (18)$$

C. INCREASE OF THE SIR WITH THE INCREASE OF N_r

Two channel realizations are considered. The first one is between the transmitter and a BS equipped with N_r receive antennas. The second realization is between the transmitter and a BS equipped with $(N_r + 1)$ receive antennas and is independent from the first realization. According to (14), with these two channel realizations, the SIR with $(N_r + 1)$ receive antennas is greater than the SIR with N_r receive antennas ($\gamma^{(N_r+1)} > \gamma^{(N_r)}$) if, and only if:

$$\left\|\mathbf{H}_0^{(N_r+1)}\right\|^4 \left(\sum_{p\in\Omega_p^*}\left|\left(\mathbf{H}_0^{(N_r)}\right)^H \mathbf{H}_p^{(N_r)}\right|^2\right) > \left\|\mathbf{H}_0^{(N_r)}\right\|^4 \left(\sum_{p\in\Omega_p^*}\left|\left(\mathbf{H}_0^{(N_r+1)}\right)^H \mathbf{H}_p^{(N_r+1)}\right|^2\right). \quad (19)$$

By considering now a large number of channel realizations, the SIR with $(N_r + 1)$ receive antennas is statistically greater than the SIR with N_r receive antennas, if and only if:

$$E\left[\left\|\mathbf{H}_0^{(N_r+1)}\right\|^4\right]\left(\sum_{p\in\Omega_p^*} E\left[\left|\left(\mathbf{H}_0^{(N_r)}\right)^H \mathbf{H}_p^{(N_r)}\right|^2\right]\right) > E\left[\left\|\mathbf{H}_0^{(N_r)}\right\|^4\right]\left(\sum_{p\in\Omega_p^*} E\left[\left|\left(\mathbf{H}_0^{(N_r+1)}\right)^H \mathbf{H}_p^{(N_r+1)}\right|^2\right]\right). \quad (20)$$

Equivalently, the SIR statistically grows as N_r increases if, and only if the propagation channel fulfills the inequation (20). This leads to the following Proposition.

Proposition 1: The SIR statistically grows with the increase of N_r if, and only if:

$$\gamma_\infty > \Gamma_{ref}, \quad (21)$$

with:

$$\Gamma_{ref} = \frac{E_0^{(2)}}{\sum_{p\in\Omega_p^*} E_p^{(2)}}, \quad (22)$$

and:

$$E_p^{(2)} = E\left[\left|\left(H_0^{n_r}\right)^* H_p^{n_r}\right|^2\right]. \quad (23)$$

Proof: See appendix A. □

One can notice that the values of γ_∞ and Γ_{ref} do not depend on N_r but only on the statistical channel properties $E_p^{(1)}$ and $E_p^{(2)}$ defined respectively in (18) and (23).

IV. STATISTICAL ANALYSIS OF THE CHANNEL COMPONENTS

Both the expression of γ_∞ in (17) and Proposition 1 rely on the statistical channel properties $E_p^{(1)}$ and $E_p^{(2)}$, defined respectively in (18) and (23). This part aims at finding their analytical value. To this end, a statistical analysis of the variables $H_p^{n_r}$ is first carried out in part IV-A by modeling the

Doppler effect with a sum-of-sinusoid method, as proposed in [32]. Then, the analytical expressions of $E_p^{(1)}$ and $E_p^{(2)}$ are given, respectively in part IV-B and IV-C. As $E_p^{(1)}$ and $E_p^{(2)}$ do not depend on the considered receive antenna and for the sake of clarity, the index n_r is removed in this part and $H_p^{n_r}$ becomes H_p.

A. STATISTICAL ANALYSIS OF H_p

The channel components H_p with $p \in \Omega_p$ are studied here. The propagation channel is modeled by the sum-of-sinusoid method defined in [32]. Indeed, the authors show that this method is useful to design and simulate Rayleigh fading channels and MIMO channels. In practice, this sum-of-sinusoid method is used in the communication system toolbox™ of the simulation environment MATLAB® [33]. Thereby:

$$h_l(t) = \sqrt{\frac{P_l}{N_l}}\left(\sum_{n=1}^{N_l}\cos\left(2\pi f_{l,n}^{(1)}t+\theta_{l,n}^{(1)}\right)\right) + j\sqrt{\frac{P_l}{N_l}}\left(\sum_{n=1}^{N_l}\cos\left(2\pi f_{l,n}^{(2)}t+\theta_{l,n}^{(2)}\right)\right), \quad (24)$$

with P_l being the average power of the l^{th} path, N_l the considered number of sinusoids for the l^{th} path, $\theta_{l,n}^{(1)}$ and $\theta_{l,n}^{(2)}$ two independent random variables having a uniform distribution over the interval $]0, 2\pi]$ and $f_{l,n}^{(i)}$ defined as follows:

$$f_{l,n}^{(i)} = f_D^{max}\cos\left(\frac{\pi}{2N_l}\left(n-\frac{1}{2}\right)+(-1)^{i-1}\frac{\pi}{4N_l}\frac{l}{L_h+2}\right), \quad (25)$$

f_D^{max} being the maximum Doppler frequency. This value is related to the speed of the user v according to:

$$f_D^{max} = \frac{v}{c}F_c, \quad (26)$$

with $c = 3.10^8$ m/s being the speed of light and F_c being the central frequency. Therefore, the higher the speed of the user v, the higher the maximum Doppler frequency f_D^{max}.

For the sake of clarity, the mathematical set of integer $\Omega_{l,n}$ is defined as follow:

$$\Omega_{l,n} = \left\{(l,n) \in \mathbb{N}^2 \mid 0 \le l \le (L_h-1) \text{ and } 1 \le n \le N_l\right\}. \quad (27)$$

Moreover, the following variables are given:

$$\alpha_l = \frac{P_l}{4N_l}, \quad (28)$$

and:

$$\begin{cases}\theta_{l,n} = \left(\pi\dfrac{f_{l,n}^{(1)}}{F_0}+\theta_{l,n}^{(1)}\right) \bmod 2\pi \\ \theta'_{l,n} = \left(\pi\dfrac{f_{l,n}^{(2)}}{F_0}+\theta_{l,n}^{(2)}\right) \bmod 2\pi.\end{cases} \quad (29)$$

As $\theta_{l,n}^{(1)}$ and $\theta_{l,n}^{(2)}$ are two independent random variables having a uniform distribution over the interval $]0, 2\pi]$, $\theta_{l,n}$ and $\theta'_{l,n}$ are also two independent random variables having a uniform distribution over the interval $]0, 2\pi]$. Finally, the following variables are defined:

$$\begin{cases}S_{p,l,n}^{-} = \text{sinc}\left(p-\dfrac{f_{l,n}^{(1)}}{F_0}\right) \\ S_{p,l,n}^{+} = \text{sinc}\left(p+\dfrac{f_{l,n}^{(1)}}{F_0}\right) \\ S_{p,l,n}^{-'} = \text{sinc}\left(p-\dfrac{f_{l,n}^{(2)}}{F_0}\right) \\ S_{p,l,n}^{+'} = \text{sinc}\left(p+\dfrac{f_{l,n}^{(2)}}{F_0}\right).\end{cases} \quad (30)$$

Thus, the development in Appendix B shows that the components H_p can be defined by:

$$H_p = \sum_{(l,n)\in\Omega_{l,n}} H_{p,l,n}, \quad (31)$$

with:

$$\begin{aligned}H_{p,l,n} = {} & \sqrt{\alpha_l}(-1)^p e^{-j2\pi(m_0-p)F_0\tau_l} \\ & \times\left(S_{p,l,n}^{-}e^{j\theta_{l,n}}+S_{p,l,n}^{+}e^{-j\theta_{l,n}}\right) \\ & + j\sqrt{\alpha_l}(-1)^p e^{-j2\pi(m_0-p)F_0\tau_l} \\ & \times\left(S_{p,l,n}^{-'}e^{j\theta'_{l,n}}+S_{p,l,n}^{+'}e^{-j\theta'_{l,n}}\right). \end{aligned} \quad (32)$$

As sinc(x) is an even function, one can notice that:

$$\begin{cases}S_{0,l,n}^{-} = S_{0,l,n}^{+} = S_{0,l,n} = \text{sinc}\left(\dfrac{f_{l,n}^{(1)}}{F_0}\right) \\ S_{0,l,n}^{-'} = S_{0,l,n}^{+'} = S'_{0,l,n} = \text{sinc}\left(\dfrac{f_{l,n}^{(2)}}{F_0}\right).\end{cases} \quad (33)$$

According to (33), when $p = 0$ the equation (32) becomes:

$$\begin{aligned}H_{0,l,n} = {} & 2\sqrt{\alpha_l}S_{0,l,n}\cos\left(\theta_{l,n}\right)e^{-j2\pi m_0F_0\tau_l} \\ & + 2j\sqrt{\alpha_l}S'_{0,l,n}\cos\left(\theta'_{l,n}\right)e^{-j2\pi m_0F_0\tau_l}. \end{aligned} \quad (34)$$

One can see that $H_{p,l,n}$ and $H_{p',l',n'}$ are independent variables if $(l,n) \neq (l',n')$. Moreover, as:

$$E\left[e^{\pm j\theta_{l,n}}\right] = E\left[e^{\pm j\theta'_{l,n}}\right] = 0, \quad (35)$$

it comes:

$$E\left[H_{p,l,n}\right] = 0, \quad (36)$$

$\forall(l,n) \in \Omega_{l,n}$ and $\forall p \in \Omega_p$.

B. EXPRESSION OF $E_p^{(1)}$

The expression of $E_p^{(1)} = E\left[H_0^* H_p\right]$ is now deduced from (31), (32) and (34). Firstly, using (31) $E_p^{(1)}$ becomes:

$$E_p^{(1)} = \sum_{(l,n)\in\Omega_{l,n}}\sum_{(l',n')\in\Omega_{l,n}} E\left[H_{0,l,n}^* H_{p,l',n'}\right]. \quad (37)$$

As $H_{p,l,n}$ and $H_{p',l',n'}$ are independent variables if $(l,n) \neq (l',n')$ and according to (36), the equation (37) becomes:

$$E_p^{(1)} = \sum_{(l,n)\in\Omega_{l,n}} E\left[H_{0,l,n}^* H_{p,l,n}\right]. \tag{38}$$

Then, using the development in Appendix C, the equation (38) becomes:

$$\begin{aligned} E_p^{(1)} = (-1)^p \sum_{(l,n)\in\Omega_{l,n}} \alpha_l S_{0,l,n} \left(S_{p,l,n}^- + S_{p,l,n}^+\right) e^{j2\pi p F_0 \tau_l} \\ + (-1)^p \sum_{(l,n)\in\Omega_{l,n}} \alpha_l S'_{0,l,n} \left(S_{p,l,n}^{-'} + S_{p,l,n}^{+'}\right) e^{j2\pi p F_0 \tau_l}. \end{aligned} \tag{39}$$

Finally, according to (33), when $p = 0$, $E_p^{(1)}$ becomes:

$$E_0^{(1)} = \sum_{(l,n)\in\Omega_{l,n}} 2\alpha_l \left(\left(S_{0,l,n}\right)^2 + \left(S'_{0,l,n}\right)^2\right). \tag{40}$$

C. EXPRESSION OF $E_p^{(2)}$

The expression of $E_p^{(2)} = E\left[\left|H_0^* H_p\right|^2\right]$ is deduced from (31), (32) and (34). Firstly, using (31), $E_p^{(2)}$ becomes:

$$\begin{aligned} E_p^{(2)} = &\sum\nolimits_{(l_1,n_1)\in\Omega_{l,n}} \sum\nolimits_{(l_2,n_2)\in\Omega_{l,n}} \\ &\times \sum\nolimits_{(l_3,n_3)\in\Omega_{l,n}} \sum\nolimits_{(l_4,n_4)\in\Omega_{l,n}} \\ &\times E\left[H_{0,l_1,n_1}^* H_{p,l_2,n_2} H_{0,l_3,n_3} H_{p,l_4,n_4}^*\right]. \end{aligned} \tag{41}$$

As $H_{p,l,n}$ and $H_{p',l',n'}$ are independent variables if $(l,n) \neq (l',n')$ and according to (36):

$$E\left[H_{0,l_1,n_1}^* H_{p,l_2,n_2} H_{0,l_3,n_3} H_{p,l_4,n_4}^*\right] = 0, \tag{42}$$

if one of the following cases is verified:

$$\begin{cases} (l_1,n_1) \notin \{(l_2,n_2),(l_3,n_3),(l_4,n_4)\} \\ (l_2,n_2) \notin \{(l_1,n_1),(l_3,n_3),(l_4,n_4)\} \\ (l_3,n_3) \notin \{(l_1,n_1),(l_2,n_2),(l_4,n_4)\} \\ (l_4,n_4) \notin \{(l_1,n_1),(l_2,n_2),(l_3,n_3)\}. \end{cases} \tag{43}$$

Therefore, (41) can be simplified as follows:

$$\begin{aligned} E_p^{(2)} = &\sum\nolimits_{(l,n)\in\Omega_{l,n}} E\left[\left|H_{0,l,n}^* H_{p,l,n}\right|^2\right] \\ &+ \sum\nolimits_{(l,n)\in\Omega_{l,n}} \sum\nolimits_{(l',n')\in\{\Omega_{l,n}\setminus(l,n)\}} \\ &\times E\left[\left|H_{0,l,n}\right|^2\right] E\left[\left|H_{p,l',n'}\right|^2\right] \\ &+ \sum\nolimits_{(l,n)\in\Omega_{l,n}} \sum\nolimits_{(l',n')\in\{\Omega_{l,n}\setminus(l,n)\}} \\ &\times E\left[H_{0,l,n}^* H_{p,l,n}\right] E\left[H_{0,l',n'}^* H_{p,l',n'}\right]^* \\ &+ \sum\nolimits_{(l,n)\in\Omega_{l,n}} \sum\nolimits_{(l',n')\in\{\Omega_{l,n}\setminus(l,n)\}} \\ &\times E\left[H_{0,l,n} H_{p,l,n}\right] E\left[H_{0,l',n'} H_{p,l',n'}\right]^*, \end{aligned} \tag{44}$$

or equivalently:

$$\begin{aligned} E_p^{(2)} = &\sum_{(l,n)\in\Omega_{l,n}} E\left[\left|H_{0,l,n}^* H_{p,l,n}\right|^2\right] \\ &- E\left[\left|H_{0,l,n}\right|^2\right] E\left[\left|H_{p,l,n}\right|^2\right] - \left|E\left[H_{0,l,n}^* H_{p,l,n}\right]\right|^2 \\ &- \left|E\left[H_{0,l,n} H_{p,l,n}\right]\right|^2 + \left(\sum_{(l,n)\in\Omega_{l,n}} E\left[\left|H_{0,l,n}\right|^2\right]\right) \\ &\times \left(\sum_{(l,n)\in\Omega_{l,n}} E\left[\left|H_{p,l,n}\right|^2\right]\right) \\ &+ \left|\sum_{(l,n)\in\Omega_{l,n}} E\left[H_{0,l,n}^* H_{p,l,n}\right]\right|^2 \\ &+ \left|\sum_{(l,n)\in\Omega_{l,n}} E\left[H_{0,l,n} H_{p,l,n}\right]\right|^2. \end{aligned} \tag{45}$$

Therefore, the development in Appendix D gives the equation (46), as shown at the bottom of the next page. According to (33), when $p = 0$, $E_p^{(2)}$ becomes:

$$\begin{aligned} E_0^{(2)} = &\sum_{(l,n)\in\Omega_{l,n}} -6\alpha_l^2 \left(\left(S_{0,l,n}\right)^4 + \left(S'_{0,l,n}\right)^4\right) \\ &+ 2\left(\sum_{(l,n)\in\Omega_{l,n}} 2\,\alpha_l \left(\left(S_{0,l,n}\right)^2 + \left(S'_{0,l,n}\right)^2\right)\right)^2 \\ &+ \left|\sum_{(l,n)\in\Omega_{l,n}} 2\alpha_l \left(\left(S_{0,l,n}\right)^2 - \left(S'_{0,l,n}\right)^2\right) e^{-j4\pi m_0 F_0 \tau_l}\right|^2. \end{aligned} \tag{47}$$

Thanks to the equation (39) and (46), the statistical variables $E_p^{(1)}$ and $E_p^{(2)}$ can be computed knowing the average power of each multipath component P_l, the normalized delay of each multipath component $(\tau_l.F_0)$, the normalized maximum Doppler frequency (f_D^{max}/F_0) and the sub-carrier index m_0 (only for $E_p^{(2)}$). Thereby, the value of γ_∞ and Γ_{ref} can be computed by simply knowing the channel properties P_l, $(\tau_l.F_0)$, (f_D^{max}/F_0) and m_0 (only for Γ_{ref}). Thus, Proposition 1 can be easily verified whatever the channel model.

V. SIMULATIONS

In this part, the SIR and the BER with channel coding are evaluated thanks to simulations in order to verify the analytical results and to visualize the impact of the Doppler effect as a function of the number of receive antennas. The simulation results are shown in part V-A for the SIR and in part V-B for the BER.

A. SIR

For the evaluation of the SIR, the set of useful sub-carriers considered is $\Omega_p = [-300\ ,\ 300]$. Moreover, three channel

models are investigated. The first one is a single-path propagation channel, meaning $L_h = 1$, $P_0 = 0$ dB and $\tau_0 = 0$ s. With such a propagation channel, the expressions of $E_p^{(1)}$ and $E_p^{(2)}$, respectively in (39) and (46), only rely on the normalized maximum Doppler frequency (f_D^{max}/F_0). Additionally, two multi-path channel models are also considered, namely the Extended Vehicular A (EVA) and Extended Typical Urban (ETU) channel models defined in [34] and [35]. Their delays τ_l and corresponding average powers P_l are given in Table 1. For these channel models, the inter-carrier spacing is set to $F_0 = 15$ kHz and the considered sub-carrier index is $m_0 = 512$. Finally, the FFT size of the OFDM modulation for the simulations is set to $M = 1024$, the CP length is equal to 7% of the symbol length and the number of sinusoids for the analytical results is set to $N_l = 30, \forall l \in [0\ ,\ L_h - 1]$, as it is the maximum value considered in [32].

TABLE 1. EVA and ETU channel models.

	EVA		ETU	
l	τ_l (ns)	P_l (dB)	τ_l (ns)	P_l (dB)
0	0	0.0	0	-1.0
1	30	-1.5	50	-1.0
2	150	-1.4	120	-1.0
3	310	-3.6	200	0.0
4	370	-0.6	230	0.0
5	710	-9.1	500	0.0
6	1090	-7.0	1600	-3.0
7	1730	-12.0	2300	-5.0
8	2510	-16.9	5000	-7.0

In Figs. 3, 4 and 5, the SIR is drawn as a function of the normalized maximum Doppler frequency (f_D^{max}/F_0) respectively for the single-path, EVA and ETU channel models and for 2, 8, 32 and 128 receive antennas. In order to verify the equation (17) and Proposition 1, the value of γ_∞ and Γ_{ref} are also given in these Figures.

As expected, by looking at the red plain line, the asymptotic SIR γ_∞ defined in (17) decreases with the increase of the normalized maximum Doppler frequency. Indeed, the greater the normalized maximum Doppler frequency, the greater the impact of the Doppler effect.

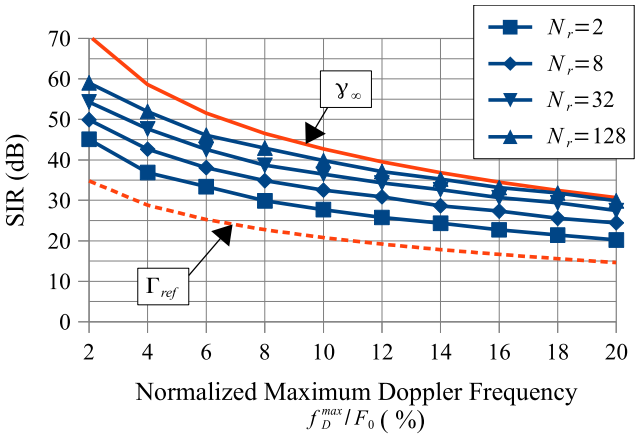

FIGURE 3. γ_∞, Γ_{ref} and simulated SIR as a function of the normalized maximum Doppler frequency (f_D^{max}/F_0) for the single-path channel model.

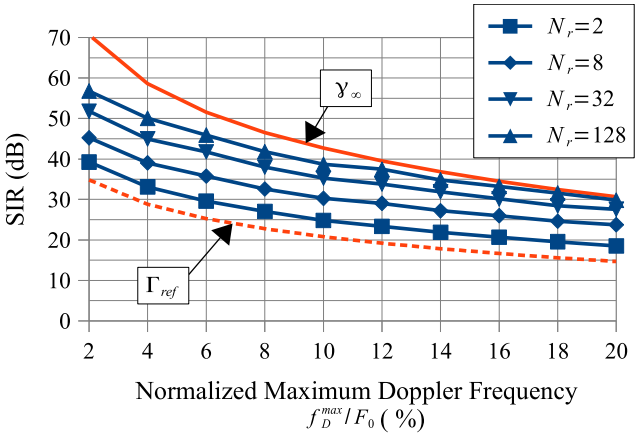

FIGURE 4. γ_∞, Γ_{ref} and simulated SIR as a function of the normalized maximum Doppler frequency (f_D^{max}/F_0) for the EVA channel model.

$$
\begin{aligned}
E_p^{(2)} = & \left(\sum_{(l,n)\in\Omega_{l,n}} -2\alpha_l^2 \left(S_{0,l,n}\right)^2 \left(\left(S_{p,l,n}^{-}\right)^2 + \left(S_{p,l,n}^{+}\right)^2 + S_{p,l,n}^{-} S_{p,l,n}^{+} \right) \right) \\
& + \left(\sum_{(l,n)\in\Omega_{l,n}} -2\alpha_l^2 \left(S'_{0,l,n}\right)^2 \left(\left(S_{p,l,n}^{-'}\right)^2 + \left(S_{p,l,n}^{+'}\right)^2 + S_{p,l,n}^{-'} S_{p,l,n}^{+'} \right) \right) \\
& + \left(\sum_{(l,n)\in\Omega_{l,n}} 2\alpha_l \left(\left(S_{0,l,n}\right)^2 + \left(S'_{0,l,n}\right)^2 \right) \right) \left(\sum_{(l,n)\in\Omega_{l,n}} \alpha_l \left(\left(S_{p,l,n}^{-}\right)^2 + \left(S_{p,l,n}^{+}\right)^2 + \left(S_{p,l,n}^{-'}\right)^2 + \left(S_{p,l,n}^{+'}\right)^2 \right) \right) \\
& + \left| \sum_{(l,n)\in\Omega_{l,n}} \alpha_l \left(S_{0,l,n} \left(S_{p,l,n}^{-} + S_{p,l,n}^{+} \right) + S'_{0,l,n} \left(S_{p,l,n}^{-'} + S_{p,l,n}^{+'} \right) \right) e^{j2\pi p F_0 \tau_l} \right|^2 \\
& + \left| \sum_{(l,n)\in\Omega_{l,n}} \alpha_l \left(S_{0,l,n} \left(S_{p,l,n}^{-} + S_{p,l,n}^{+} \right) - S'_{0,l,n} \left(S_{p,l,n}^{-'} + S_{p,l,n}^{+'} \right) \right) e^{-j2\pi (2m_0 - p) F_0 \tau_l} \right|^2
\end{aligned}
\tag{46}
$$

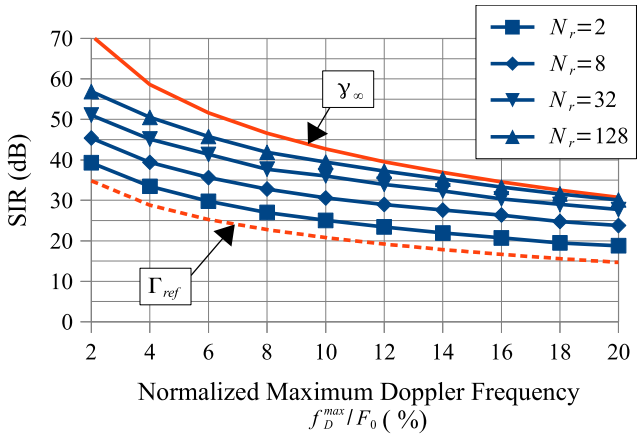

FIGURE 5. γ_∞, Γ_{ref} and simulated SIR as a function of the normalized maximum Doppler frequency (f_D^{max}/F_0) for the ETU channel model.

We remark that the value of γ_∞ is similar whatever the channel model (single-path, EVA or ETU). Therefore, the impact of the frequency selectivity of the channel on the value of γ_∞ seems to be negligible. This result is in line with that from [19], where the author stated that the effect of the frequency selectivity of the channel vanishes in the limit of an infinite number of antennas. The asymptotic SIR is thus approximately equal to 43 dB when $f_D^{max}/F_0 = 10\%$ and decreases up to 30 dB when f_D^{max}/F_0 reaches 20% whatever the channel model.

The comparison between the red plain line (γ_∞) and the red dashed line (Γ_{ref}) aims at verifying Proposition 1. As for the asymptotic SIR, the value of Γ_{ref} is similar whatever the channel model (single-path, EVA or ETU) and thus the impact of the frequency selectivity of the channel on the value of Γ_{ref} seems to be negligible. Moreover, γ_∞ is always greater than Γ_{ref}. Proposition 1 is thus verified and the SIR should increase with the increase of the number of receive antennas N_r whatever the channel model. Therefore, this result proves that a massive MIMO system with a large number of antennas on the BS side can be used to reduce the impact of the Doppler effect.

These theoretical results are confirmed by the simulation results given by the blue lines in Figs. 3, 4 and 5. As expected, the SIR always increases with the increase of N_r. This increase is significant. For example, there is a gain of approximately 5 dB between a system with $N_r = 8$ receive antennas and a system with $N_r = 32$ receive antennas. Finally, as the number of receive antennas increases, the blue lines seem to tend towards the red plain line which confirms the expression of γ_∞ in (17).

B. BER

The BER with channel coding is now evaluated in this part in order to visualize the impact of the Doppler effect as a function of the number of receive antennas from a more practical point of view. The EVA and ETU channel models described in Table 1 are used in this part. Moreover, the FFT size is set to M = 1024, the subcarrier spacing is set to $F_0 = 15$ kHz and the CP length is equal to 7% of the symbol length as in the previous part. A turbo-code is used with a coding rate of 0.75 and 64QAM symbols. The maximum Doppler frequency is arbitrary high in order to visualize the impact of the Doppler effect, meaning $f_D^{max} = 3000$ Hz. It corresponds to normalized maximum Doppler frequency (f_D^{max}/F_0) equal to 20% and, according to (26), to a speed of $v = 540$ km/h with a central frequency of $F_c = 6$ GHz.

In Figs. 6 and 7, the BER with channel coding is drawn as a function of the SNR respectively for the EVA and ETU channel models and for 1, 4, 16 and 64 receive antennas. The BER with channel coding of a Single-Input Single-Output (SISO) system on a Gaussian channel without mobility is also added on these Figs. to serve as a baseline.

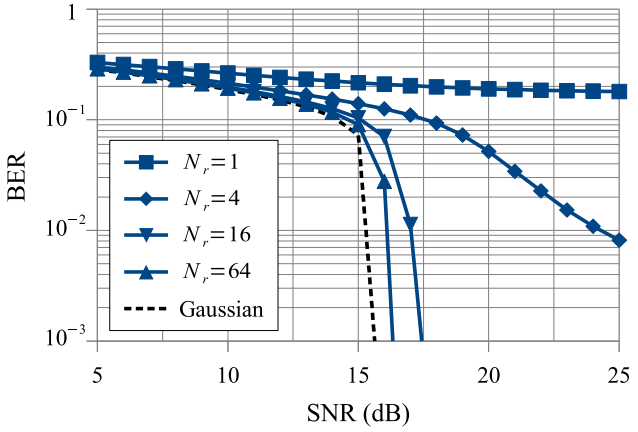

FIGURE 6. BER with channel coding as a function of the SNR for the EVA channel model.

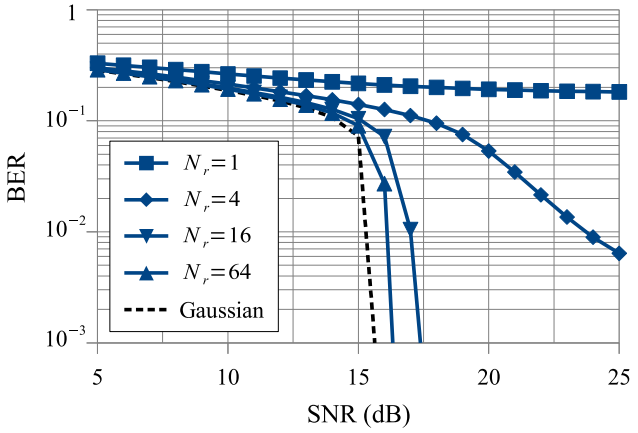

FIGURE 7. BER with channel coding as a function of the SNR for the ETU channel model.

Firstly, Figs. 6 and 7 show that the Doppler effect has a strong impact on the performance of the system when a single antenna is used on the BS side. Indeed, an error floor higher

than 10^{-1} appears when $N_r = 1$. However, as expected the increase of the number of receive antennas induces a reduction of the impact of the Doppler effect and thereby an improvement of the performance in terms of BER. Thus, when the number of antennas increases, the performance of the proposed system with mobility tends to the performance of a SISO system on a Gaussian channel without mobility. Finally, Figs. 6 and 7 show that the impact of the Doppler effect can be highly reduced even with a relatively low number of receive antennas. Indeed, with only $N_r = 16$ receive antennas no error floor appears and the BER curve is separated from the one on a Gaussian channel by only 4 dB.

VI. CONCLUSION

The effect of a very large number of uncorrelated receive antennas on the ICI due to the Doppler effect has been studied in this paper considering an OFDM communication with a simple MRC receiver. Relaying on analytical and simulation results, the contribution of this paper is twofold. Firstly, the asymptotic value of the SIR, when the number of receive antennas tends towards the infinity, has been analytically expressed. Secondly, it was proven that increasing the number of receive antennas allows for reducing the interference due to the Doppler effect. Finally, the simulation results show that this reduction is significant in practice even with a relatively low number of receive antennas.

This study helps to better evaluate the benefits of massive MIMO systems for 5G in the presence of mobility. From a more practical point of view, this paper highlights the ability to improve the performance of V2x communications when using a massive MIMO system with a low-complexity MRC receiver.

The results of this contribution are based on some assumptions corresponding to a case untreated in the literature and this paper paves the way for further studies regarding the following aspects.

- Considering a communication with a LOS component, a Doppler shift adds to the Doppler spread. Therefore, the impact of a massive MIMO receiver on this Doppler shift component could be studied using a Rician fading channel model instead of a Rayleigh fading channel model.
- This contribution can be extended with multi-user communications, using a Zero Forcing (ZF) technique or a Minimum Mean Square Error (MMSE) technique.
- It would be interesting to extend this work with a geometry-based channel model. This type of channel model is more difficult to analytically study but it takes into account the correlation between the antennas and it is more accurate to represent high mobility propagation environments.

All these aspects are potential approaches for future contributions.

APPENDIX A
PROOF OF PROPOSITION 1

With non-correlated antennas, it can be seen that:

$$\begin{aligned} &E\left[\left|\left(\mathbf{H}_0^{(N_r)}\right)^H \mathbf{H}_p^{(N_r)}\right|^2\right] \\ &= E\left[\left|\sum_{n_r=0}^{N_r-1}\left(H_0^{n_r}\right)^* H_p^{n_r}\right|^2\right] \\ &= N_r E\left[\left|\left(H_0^{n_r}\right)^* H_p^{n_r}\right|^2\right] \\ &\quad + N_r(N_r-1)\left|E\left[\left(H_0^{n_r}\right)^* H_p^{n_r}\right]\right|^2 \\ &= N_r E_p^{(2)} + N_r(N_r-1)\left|E_p^{(1)}\right|^2. \end{aligned} \tag{48}$$

Then, the special case where $p = 0$ gives:

$$E\left[\left\|\mathbf{H}_0^{(N_r)}\right\|^4\right] = N_r E_0^{(2)} + N_r(N_r-1)\left|E_0^{(1)}\right|^2. \tag{49}$$

With $(N_r + 1)$ receive antennas, the equation (48) becomes:

$$\begin{aligned} E\left[\left|\left(\mathbf{H}_0^{(N_r+1)}\right)^H \mathbf{H}_p^{(N_r+1)}\right|^2\right] &= (N_r+1)E_p^{(2)} \\ &\quad + (N_r+1)N_r\left|E_p^{(1)}\right|^2, \end{aligned} \tag{50}$$

and when $p = 0$:

$$E\left[\left\|\mathbf{H}_0^{(N_r+1)}\right\|^4\right] = (N_r+1)E_0^{(2)} + (N_r+1)N_r\left|E_0^{(1)}\right|^2. \tag{51}$$

Using (48), (49), (50) and (51), the inequation (20) becomes:

$$\begin{aligned} &\left((N_r+1)E_0^{(2)} + (N_r+1)N_r\left|E_0^{(1)}\right|^2\right) \\ &\quad \times \sum_{p\in\Omega_p^*}\left(N_r E_p^{(2)} + N_r(N_r-1)\left|E_p^{(1)}\right|^2\right) \\ &> \left(N_r E_0^{(2)} + N_r(N_r-1)\left|E_0^{(1)}\right|^2\right) \\ &\quad \times \sum_{p\in\Omega_p^*}\left((N_r+1)E_p^{(2)} + (N_r+1)N_r\left|E_p^{(1)}\right|^2\right). \end{aligned} \tag{52}$$

Divided by $N_r(N_r + 1)$, the inequation (52) becomes:

$$\begin{aligned} &\left(E_0^{(2)} + N_r\left|E_0^{(1)}\right|^2\right) \times \sum_{p\in\Omega_p^*}\left(E_p^{(2)} + (N_r-1)\left|E_p^{(1)}\right|^2\right) \\ &> \left(E_0^{(2)} + (N_r-1)\left|E_0^{(1)}\right|^2\right) \times \sum_{p\in\Omega_p^*}\left(E_p^{(2)} + N_r\left|E_p^{(1)}\right|^2\right). \end{aligned} \tag{53}$$

Then, subtracting

$$\left(E_0^{(2)} + N_r\left|E_0^{(1)}\right|^2\right)\left(\sum_{p\in\Omega_p^*}\left(E_p^{(2)} + N_r\left|E_p^{(1)}\right|^2\right)\right)$$

on both sides of (53), it comes:

$$\left(E_0^{(2)} + N_r \left|E_0^{(1)}\right|^2\right)\left(\sum_{p\in\Omega_p^*} - \left|E_p^{(1)}\right|^2\right) > \left(-\left|E_0^{(1)}\right|^2\right)\left(\sum_{p\in\Omega_p^*}\left(E_p^{(2)} + N_r\left|E_p^{(1)}\right|^2\right)\right). \quad (54)$$

Finally, adding $N_r\left|E_0^{(1)}\right|^2\left(\sum_{p\in\Omega_p^*}\left|E_p^{(1)}\right|^2\right)$, (54) becomes:

$$E_0^{(2)}\left(\sum_{p\in\Omega_p^*} - \left|E_p^{(1)}\right|^2\right) > \left(-\left|E_0^{(1)}\right|^2\right)\left(\sum_{p\in\Omega_p^*} E_p^{(2)}\right). \quad (55)$$

which is equivalent to:

$$\frac{\left|E_0^{(1)}\right|^2}{\sum_{p\in\Omega_p^*}\left|E_p^{(1)}\right|^2} > \frac{E_0^{(2)}}{\sum_{p\in\Omega_p^*} E_p^{(2)}}. \quad (56)$$

APPENDIX B
DEVELOPMENT OF H_p

Using (24) in (9) the components H_p can be described as follows:

$$H_p = \sum_{(l,n)\in\Omega_{l,n}} H_{p,l,n}, \quad (57)$$

with:

$$H_{p,l,n} = \sqrt{\frac{P_l}{N_l}}F_0\left(\int_0^{1/F_0}\cos\left(2\pi f_{l,n}^{(1)}t + \theta_{l,n}^{(1)}\right)e^{-j2\pi pF_0t}dt\right) \times \exp\left[-j2\pi(m_0-p)F_0\tau_l\right] + j\sqrt{\frac{P_l}{N_l}}F_0\left(\int_0^{1/F_0}\cos\left(2\pi f_{l,n}^{(2)}t + \theta_{l,n}^{(2)}\right)e^{-j2\pi pF_0t}dt\right) \times \exp\left[-j2\pi(m_0-p)F_0\tau_l\right]. \quad (58)$$

Using the Fourier transform, the equation (58) becomes:

$$H_{p,l,n} = \sqrt{\frac{P_l}{N_l}}F_0\exp\left[-j2\pi(m_0-p)F_0\tau_l\right] \times \mathcal{F}_{f=pF_0}\left[\cos\left(2\pi f_{l,n}^{(1)}t + \theta_{l,n}^{(1)}\right).\Pi_{1/F_0}\left(t-\frac{1}{2F_0}\right)\right] + j\sqrt{\frac{P_l}{N_l}}F_0\exp\left[-j2\pi(m_0-p)F_0\tau_l\right] \times \mathcal{F}_{f=pF_0}\left[\cos\left(2\pi f_{l,n}^{(1)}t + \theta_{l,n}^{(1)}\right).\Pi_{1/F_0}\left(t-\frac{1}{2F_0}\right)\right], \quad (59)$$

with:

$$\Pi_{1/F_0}(t) = \begin{cases} 1, & if\ |t| < \dfrac{1}{2F_0} \\ 0, & if\ |t| > \dfrac{1}{2F_0}. \end{cases} \quad (60)$$

As:

$$\begin{aligned}\mathcal{F}\left[\cos\left(2\pi f_{l,n}^{(i)}t + \theta_{l,n}^{(i)}\right)\right] &= \mathcal{F}\left[\cos\left(2\pi f_{l,n}^{(i)}\left(t + \frac{\theta_{l,n}^{(i)}}{2\pi f_{l,n}^{(i)}}\right)\right)\right] \\ &= \frac{1}{2}\left(\delta\left(f - f_{l,n}^{(i)}\right) + \delta\left(f + f_{l,n}^{(i)}\right)\right)e^{j2\pi f\frac{\theta_{l,n}^{(i)}}{2\pi f_{l,n}^{(i)}}} \\ &= \frac{1}{2}\left(e^{j\theta_{l,n}^{(i)}}\delta\left(f - f_{l,n}^{(i)}\right) + e^{-j\theta_{l,n}^{(i)}}\delta\left(f + f_{l,n}^{(i)}\right)\right) \quad (61)\end{aligned}$$

and as:

$$\mathcal{F}\left[\Pi_{1/F_0}\left(t-\frac{1}{2F_0}\right)\right] = \frac{1}{F_0}\text{sinc}\left(\frac{f}{F_0}\right)e^{-j2\pi\frac{f}{2F_0}}, \quad (62)$$

it comes:

$$\mathcal{F}\left[\cos\left(2\pi f_{l,n}^{(i)}t + \theta_{l,n}^{(i)}\right).\Pi_{1/F_0}\left(t-\frac{1}{2F_0}\right)\right] = \mathcal{F}\left[\cos\left(2\pi f_{l,n}^{(i)}t + \theta_{l,n}^{(i)}\right)\right] * \mathcal{F}\left[\Pi_{1/F_0}\left(t-\frac{1}{2F_0}\right)\right] \quad (63)$$

and thus:

$$\begin{aligned}&\mathcal{F}_{f=pF_0}\left[\cos\left(2\pi f_{l,n}^{(i)}t + \theta_{l,n}^{(i)}\right).\Pi_{1/F_0}\left(t-\frac{1}{2F_0}\right)\right] \\ &= \int_{-\infty}^{+\infty}\frac{1}{2}\left(e^{j\theta_{l,n}^{(i)}}\delta\left(f - f_{l,n}^{(i)}\right) + e^{-j\theta_{l,n}^{(i)}}\delta\left(f + f_{l,n}^{(i)}\right)\right) \times \frac{1}{F_0}\text{sinc}\left(\frac{pF_0 - f}{F_0}\right)e^{-j2\pi\frac{pF_0-f}{2F_0}}df \\ &= \frac{1}{2F_0}e^{-j\pi p}\text{sinc}\left(p - \frac{f_{l,n}^{(i)}}{F_0}\right)e^{j\left(\pi\frac{f_{l,n}^{(i)}}{F_0} + \theta_{l,n}^{(i)}\right)} + \frac{1}{2F_0}e^{-j\pi p}\text{sinc}\left(p + \frac{f_{l,n}^{(i)}}{F_0}\right)e^{-j\left(\pi\frac{f_{l,n}^{(i)}}{F_0} + \theta_{l,n}^{(i)}\right)}. \quad (64)\end{aligned}$$

Therefore the equation (59) becomes:

$$\begin{aligned}H_{p,l,n} = &\sqrt{\frac{P_l}{4N_l}}(-1)^p\text{sinc}\left(p - \frac{f_{l,n}^{(1)}}{F_0}\right) \times e^{j\left(\pi\frac{f_{l,n}^{(1)}}{F_0} + \theta_{l,n}^{(1)}\right)}e^{-j2\pi(m_0-p)F_0\tau_l} \\ &+ \sqrt{\frac{P_l}{4N_l}}(-1)^p\text{sinc}\left(p + \frac{f_{l,n}^{(1)}}{F_0}\right) \times e^{-j\left(\pi\frac{f_{l,n}^{(1)}}{F_0} + \theta_{l,n}^{(1)}\right)}e^{-j2\pi(m_0-p)F_0\tau_l}\end{aligned}$$

$$+j\sqrt{\frac{P_l}{4N_l}}(-1)^p \mathrm{sinc}\left(p-\frac{f_{l,n}^{(2)}}{F_0}\right) \times e^{j\left(\pi\frac{f_{l,n}^{(2)}}{F_0}+\theta_{l,n}^{(2)}\right)} e^{-j2\pi(m_0-p)F_0\tau_l} +j\sqrt{\frac{P_l}{4N_l}}(-1)^p \mathrm{sinc}\left(p+\frac{f_{l,n}^{(2)}}{F_0}\right) \times e^{-j\left(\pi\frac{f_{l,n}^{(2)}}{F_0}+\theta_{l,n}^{(2)}\right)} e^{-j2\pi(m_0-p)F_0\tau_l}. \quad (65)$$

Finally, using the notations in (28) (29) and (30), the equation (65) can be rewritten as in (32).

APPENDIX C
DEVELOPMENT OF $E_p^{(1)}$

Using (32) and (34), the expression of $H_{0,l,n}^* H_{p,l,n}$ is:

$$\begin{aligned} &H_{0,l,n}^* H_{p,l,n} \\ &= 2\alpha_l(-1)^p \left(S_{0,l,n}\cos\left(\theta_{l,n}\right) - jS'_{0,l,n}\cos\left(\theta'_{l,n}\right)\right) \\ &\quad\times \left(S_{p,l,n}^{-} e^{j\theta_{l,n}} + S_{p,l,n}^{+} e^{-j\theta_{l,n}}\right) e^{j2\pi pF_0\tau_l} \\ &\quad + 2j\alpha_l(-1)^p \left(S_{0,l,n}\cos\left(\theta_{l,n}\right) - jS'_{0,l,n}\cos\left(\theta'_{l,n}\right)\right) \\ &\quad\times \left(S_{p,l,n}^{-'} e^{j\theta'_{l,n}} + S_{p,l,n}^{+'} e^{-j\theta'_{l,n}}\right) e^{j2\pi pF_0\tau_l}. \end{aligned} \quad (66)$$

Knowing that $\theta_{l,n}$ and $\theta'_{l,n}$ are two independent random variables having a uniform distribution over the interval $]0, 2\pi]$, it comes:

$$\begin{cases} E\left[\cos\left(\theta_{l,n}\right)\right] = E\left[e^{\pm j\theta_{l,n}}\right] = 0 \\ E\left[\cos\left(\theta'_{l,n}\right)\right] = E\left[e^{\pm j\theta'_{l,n}}\right] = 0 \end{cases} \quad (67)$$

and:

$$\begin{aligned} E\left[\cos\left(\theta_{l,n}\right)e^{\pm j\theta_{l,n}}\right] &= E\left[\cos\left(\theta'_{l,n}\right)e^{\pm j\theta'_{l,n}}\right] \\ &= E\left[\frac{1}{2}\left(e^{j\theta_{l,n}} + e^{-j\theta_{l,n}}\right)e^{\pm j\theta_{l,n}}\right] \\ &= \frac{1}{2}. \end{aligned} \quad (68)$$

Therefore, the expression of $E\left[H_{0,l,n}^* H_{p,l,n}\right]$ is :

$$\begin{aligned} &E\left[H_{0,l,n}^* H_{p,l,n}\right] \\ &= \alpha_l(-1)^p S_{0,l,n}\left(S_{p,l,n}^{-} + S_{p,l,n}^{+}\right)e^{j2\pi pF_0\tau_l} \\ &\quad + \alpha_l(-1)^p S'_{0,l,n}\left(S_{p,l,n}^{-'} + S_{p,l,n}^{+'}\right)e^{j2\pi pF_0\tau_l}. \end{aligned} \quad (69)$$

APPENDIX D
DEVELOPMENT OF $E_p^{(2)}$

In order to develop $E_p^{(2)}$, the expressions of $E\left[\left|H_{p,l,n}\right|^2\right]$, $E\left[H_{0,l,n}H_{p,l,n}\right]$ and $E\left[\left|H_{0,l,n}^* H_{p,l,n}\right|^2\right]$ are first given thereafter.

Using (32), the expression of $\left|H_{p,l,n}\right|^2$ is:

$$\begin{aligned} \left|H_{p,l,n}\right|^2 &= \alpha_l\left(S_{p,l,n}^{-}e^{-j\theta_{l,n}} + S_{p,l,n}^{+}e^{j\theta_{l,n}}\right) \\ &\quad\times\left(S_{p,l,n}^{-}e^{j\theta_{l,n}} + S_{p,l,n}^{+}e^{-j\theta_{l,n}}\right) \\ &\quad + j\alpha_l\left(S_{p,l,n}^{-}e^{-j\theta_{l,n}} + S_{p,l,n}^{+}e^{j\theta_{l,n}}\right) \\ &\quad\times\left(S_{p,l,n}^{-'}e^{j\theta'_{l,n}} + S_{p,l,n}^{+'}e^{-j\theta'_{l,n}}\right) \\ &\quad - j\alpha_l\left(S_{p,l,n}^{-'}e^{-j\theta'_{l,n}} + S_{p,l,n}^{+'}e^{j\theta'_{l,n}}\right) \\ &\quad\times\left(S_{p,l,n}^{-}e^{j\theta_{l,n}} + S_{p,l,n}^{+}e^{-j\theta_{l,n}}\right) \\ &\quad + \alpha_l\left(S_{p,l,n}^{-'}e^{-j\theta'_{l,n}} + S_{p,l,n}^{+'}e^{j\theta'_{l,n}}\right) \\ &\quad\times\left(S_{p,l,n}^{-'}e^{j\theta'_{l,n}} + S_{p,l,n}^{+'}e^{-j\theta'_{l,n}}\right). \end{aligned} \quad (70)$$

As $\theta_{l,n}$ and $\theta'_{l,n}$ are two independent random variables having a uniform distribution over the interval $]0, 2\pi]$, it comes:

$$E\left[e^{\pm 2j\theta_{l,n}}\right] = E\left[e^{\pm 2j\theta'_{l,n}}\right] = 0. \quad (71)$$

Therefore, knowing (67) and (71), the expression of $E\left[\left|H_{p,l,n}\right|^2\right]$ is:

$$\begin{aligned} &E\left[\left|H_{p,l,n}\right|^2\right] \\ &= \alpha_l\left(\left(S_{p,l,n}^{-}\right)^2 + \left(S_{p,l,n}^{+}\right)^2 + \left(S_{p,l,n}^{-'}\right)^2 + \left(S_{p,l,n}^{+'}\right)^2\right). \end{aligned} \quad (72)$$

Finally, according to (33), when $p = 0$, the expression of $E\left[\left|H_{p,l,n}\right|^2\right]$ becomes:

$$E\left[\left|H_{0,l,n}\right|^2\right] = 2\alpha_l\left(\left(S_{0,l,n}\right)^2 + \left(S'_{0,l,n}\right)^2\right). \quad (73)$$

Using (32) and (34), the expression of $H_{0,l,n}H_{p,l,n}$ is:

$$\begin{aligned} &H_{0,l,n}H_{p,l,n} \\ &= 2\alpha_l(-1)^p \left(S_{0,l,n}\cos\left(\theta_{l,n}\right) + jS'_{0,l,n}\cos\left(\theta'_{l,n}\right)\right) \\ &\quad\times \left(S_{p,l,n}^{-} e^{j\theta_{l,n}} + S_{p,l,n}^{+} e^{-j\theta_{l,n}}\right) e^{-j2\pi(2m_0-p)F_0\tau_l} \\ &\quad + 2j\alpha_l(-1)^p \left(S_{0,l,n}\cos\left(\theta_{l,n}\right) + jS'_{0,l,n}\cos\left(\theta'_{l,n}\right)\right) \\ &\quad\times \left(S_{p,l,n}^{-'} e^{j\theta'_{l,n}} + S_{p,l,n}^{+'} e^{-j\theta'_{l,n}}\right) e^{-j2\pi(2m_0-p)F_0\tau_l}. \end{aligned} \quad (74)$$

Therefore, knowing that $\theta_{l,n}$ and $\theta'_{l,n}$ are two independent variables and knowing (67) and (68), the expression of $E\left[H_{0,l,n}H_{p,l,n}\right]$ is:

$$\begin{aligned} &E\left[H_{0,l,n}H_{p,l,n}\right] \\ &= \alpha_l(-1)^p S_{0,l,n}\left(S_{p,l,n}^{-} + S_{p,l,n}^{+}\right)e^{-j2\pi(2m_0-p)F_0\tau_l} \\ &\quad - \alpha_l(-1)^p S'_{0,l,n}\left(S_{p,l,n}^{-'} + S_{p,l,n}^{+'}\right)e^{-j2\pi(2m_0-p)F_0\tau_l}. \end{aligned} \quad (75)$$

Using (66), the expression of $\left|H^*_{0,l,n}H_{p,l,n}\right|^2$ is:

$$\begin{aligned}
&\left|H^*_{0,l,n}H_{p,l,n}\right|^2 \\
&= 4\alpha_l^2\left(\left(S_{0,l,n}\right)^2\cos^2\left(\theta_{l,n}\right)+\left(S'_{0,l,n}\right)^2\cos^2\left(\theta'_{l,n}\right)\right) \\
&\quad\times\left(S^-_{p,l,n}e^{-j\theta_{l,n}}+S^+_{p,l,n}e^{j\theta_{l,n}}\right) \\
&\quad\times\left(S^-_{p,l,n}e^{j\theta_{l,n}}+S^+_{p,l,n}e^{-j\theta_{l,n}}\right) \\
&\quad+4j\alpha_l^2\left(\left(S_{0,l,n}\right)^2\cos^2\left(\theta_{l,n}\right)+\left(S'_{0,l,n}\right)^2\cos^2\left(\theta'_{l,n}\right)\right) \\
&\quad\times\left(S^-_{p,l,n}e^{-j\theta_{l,n}}+S^+_{p,l,n}e^{j\theta_{l,n}}\right) \\
&\quad\times\left(S^{-'}_{p,l,n}e^{j\theta'_{l,n}}+S^{+'}_{p,l,n}e^{-j\theta'_{l,n}}\right) \\
&\quad-4j\alpha_l^2\left(\left(S_{0,l,n}\right)^2\cos^2\left(\theta_{l,n}\right)+\left(S'_{0,l,n}\right)^2\cos^2\left(\theta'_{l,n}\right)\right) \\
&\quad\times\left(S^{-'}_{p,l,n}e^{-j\theta'_{l,n}}+S^{+'}_{p,l,n}e^{j\theta'_{l,n}}\right) \\
&\quad\times\left(S^-_{p,l,n}e^{j\theta_{l,n}}+S^+_{p,l,n}e^{-j\theta_{l,n}}\right) \\
&\quad+4\alpha_l^2\left(\left(S_{0,l,n}\right)^2\cos^2\left(\theta_{l,n}\right)+\left(S'_{0,l,n}\right)^2\cos^2\left(\theta'_{l,n}\right)\right) \\
&\quad\times\left(S^{-'}_{p,l,n}e^{-j\theta'_{l,n}}+S^{+'}_{p,l,n}e^{j\theta'_{l,n}}\right) \\
&\quad\times\left(S^{-'}_{p,l,n}e^{j\theta'_{l,n}}+S^{+'}_{p,l,n}e^{-j\theta'_{l,n}}\right). \qquad (76)
\end{aligned}$$

Therefore, knowing that $\theta_{l,n}$ and $\theta'_{l,n}$ are two independent variables and knowing (67) and (71), the expression of $E\left[\left|H^*_{0,l,n}H_{p,l,n}\right|^2\right]$ becomes the equation (77), as shown at the bottom of this page.

Knowing that $\theta_{l,n}$ and $\theta'_{l,n}$ are two independent random variables having a uniform distribution over the interval $]0,\,2\pi]$, it comes:

$$E\left[\cos^2\left(\theta'_{l,n}\right)\right]=E\left[\cos^2\left(\theta_{l,n}\right)\right]=\frac{1}{2}, \qquad (78)$$

and:

$$\begin{aligned}
&E\left[\cos^2\left(\theta_{l,n}\right)e^{\pm2j\theta_{l,n}}\right] \\
&\quad=E\left[\cos^2\left(\theta'_{l,n}\right)e^{\pm2j\theta'_{l,n}}\right] \\
&\quad=E\left[\frac{1}{4}\left(e^{2j\theta_{l,n}}+e^{-2j\theta_{l,n}}+2\right)e^{\pm2j\theta_{l,n}}\right] \\
&\quad=\frac{1}{4}. \qquad (79)
\end{aligned}$$

Therefore, according to (78) and (79), (77) becomes:

$$\begin{aligned}
&E\left[\left|H^*_{0,l,n}H_{p,l,n}\right|^2\right] \\
&\quad=2\alpha_l^2\left(\left(S_{0,l,n}\right)^2+\left(S'_{0,l,n}\right)^2\right) \\
&\qquad\times\left(\left(S^-_{p,l,n}\right)^2+\left(S^+_{p,l,n}\right)^2+\left(S^{-'}_{p,l,n}\right)^2+\left(S^{+'}_{p,l,n}\right)^2\right) \\
&\qquad+2\alpha_l^2\left(\left(S_{0,l,n}\right)^2S^-_{p,l,n}S^+_{p,l,n}+\left(S'_{0,l,n}\right)^2S^{-'}_{p,l,n}S^{+'}_{p,l,n}\right). \qquad (80)
\end{aligned}$$

Using the expressions of $E\left[\left|H_{0,l,n}\right|^2\right]$ in (72) and $E\left[\left|H_{p,l,n}\right|^2\right]$ in (73), the expression of $E\left[\left|H_{0,l,n}\right|^2\right]E\left[\left|H_{p,l,n}\right|^2\right]$ can be deduced:

$$\begin{aligned}
&E\left[\left|H_{0,l,n}\right|^2\right]E\left[\left|H_{p,l,n}\right|^2\right] \\
&\quad=2\alpha_l^2\left(\left(S_{0,l,n}\right)^2+\left(S'_{0,l,n}\right)^2\right) \\
&\qquad\times\left(\left(S^-_{p,l,n}\right)^2+\left(S^+_{p,l,n}\right)^2+\left(S^{-'}_{p,l,n}\right)^2+\left(S^{+'}_{p,l,n}\right)^2\right). \qquad (81)
\end{aligned}$$

Moreover, using the expression of $E\left[H^*_{0,l,n}H_{p,l,n}\right]$ in Appendix C, the expression of $\left|E\left[H^*_{0,l,n}H_{p,l,n}\right]\right|^2$ can be deduced:

$$\begin{aligned}
&\left|E\left[H^*_{0,l,n}H_{p,l,n}\right]\right|^2 \\
&\quad=\alpha_l^2\left(S_{0,l,n}\left(S^-_{p,l,n}+S^+_{p,l,n}\right)+S'_{0,l,n}\left(S^{-'}_{p,l,n}+S^{+'}_{p,l,n}\right)\right)^2. \qquad (82)
\end{aligned}$$

Then, the expression of $E\left[H_{0,l,n}H_{p,l,n}\right]$ in equation (75) gives the following expression for $\left|E\left[H_{0,l,n}H_{p,l,n}\right]\right|^2$:

$$\begin{aligned}
&\left|E\left[H_{0,l,n}H_{p,l,n}\right]\right|^2 \\
&\quad=\alpha_l^2\left(S_{0,l,n}\left(S^-_{p,l,n}+S^+_{p,l,n}\right)-S'_{0,l,n}\left(S^{-'}_{p,l,n}+S^{+'}_{p,l,n}\right)\right)^2. \qquad (83)
\end{aligned}$$

$$\begin{aligned}
E\left[\left|H^*_{0,l,n}H_{p,l,n}\right|^2\right] &= 4\alpha_l^2\left(S_{0,l,n}\right)^2\left(\left(S^-_{p,l,n}\right)^2+\left(S^+_{p,l,n}\right)^2+\left(S^{-'}_{p,l,n}\right)^2+\left(S^{+'}_{p,l,n}\right)^2\right)E\left[\cos^2\left(\theta_{l,n}\right)\right] \\
&\quad+4\alpha_l^2\left(S_{0,l,n}\right)^2S^-_{p,l,n}S^+_{p,l,n}E\left[\cos^2\left(\theta_{l,n}\right)\left(e^{-2j\theta_{l,n}}+e^{2j\theta_{l,n}}\right)\right] \\
&\quad+4\alpha_l^2\left(S'_{0,l,n}\right)^2\left(\left(S^-_{p,l,n}\right)^2+\left(S^+_{p,l,n}\right)^2+\left(S^{-'}_{p,l,n}\right)^2+\left(S^{+'}_{p,l,n}\right)^2\right)E\left[\cos^2\left(\theta'_{l,n}\right)\right] \\
&\quad+4\alpha_l^2\left(S'_{0,l,n}\right)^2S^{-'}_{p,l,n}S^{+'}_{p,l,n}E\left[\cos^2\left(\theta'_{l,n}\right)\left(e^{-2j\theta'_{l,n}}+e^{2j\theta'_{l,n}}\right)\right] \qquad (77)
\end{aligned}$$

Therefore, using the equations (80), (81), (82) and (83), it comes:

$$\begin{aligned} & E\left[\left|H^{*}_{0,l,n}H_{p,l,n}\right|^2\right] - E\left[\left|H_{0,l,n}\right|^2\right]E\left[\left|H_{p,l,n}\right|^2\right] \\ & \quad - \left|E\left[H^{*}_{0,l,n}H_{p,l,n}\right]\right|^2 - \left|E\left[H_{0,l,n}H_{p,l,n}\right]\right|^2 \\ & \quad = 2\alpha_l^2\left(S_{0,l,n}\right)^2 S^{-}_{p,l,n}S^{+}_{p,l,n} \\ & \qquad + 2\alpha_l^2\left(S'_{0,l,n}\right)^2 S^{-'}_{p,l,n}S^{+'}_{p,l,n} \\ & \qquad - 2\alpha_l^2\left(S_{0,l,n}\right)^2\left(S^{-}_{p,l,n} + S^{+}_{p,l,n}\right)^2 \\ & \qquad - 2\alpha_l^2\left(S'_{0,l,n}\right)^2\left(S^{-'}_{p,l,n} + S^{+'}_{p,l,n}\right)^2. \end{aligned} \tag{84}$$

Finally, using (84), (72), (73), (69) and (75), the equation (45) becomes the equation (46).

REFERENCES

[1] R. El Hattach and J. Erfanian, "5G white paper," NGMN Alliance, Frankfurt, Germany, Tech. Rep., Feb. 2015. [Online]. Available: http://www.ngmn.org

[2] A. Osseiran *et al.*, "Scenarios for 5G mobile and wireless communications: The vision of the METIS project," *IEEE Commun. Mag.*, vol. 52, no. 5, pp. 26–35, May 2014.

[3] F. Schaich *et al.*, "FANTASTIC 5G: 5G—PPP project on 5G air interface below 6 GHz," Fantastic5G, Tech. Rep. [Online]. Available: http://www.fantastic5g.eu

[4] "IMT vision framework and overall objectives of the future development of IMT for 2020 and beyond," ITU-R, Geneva, Switzerland, Tech. Rep. M.2083-0, Sep. 2015. [Online]. Available: http://www.itu.int

[5] J. Li and M. Kavehrad, "Effects of time selective multipath fading on OFDM systems for broadband mobile applications," *IEEE Commun. Lett.*, vol. 3, no. 12, pp. 332–334, Dec. 1999.

[6] X. Cai and G. B. Giannakis, "Bounding performance and suppressing intercarrier interference in wireless mobile OFDM," *IEEE Trans. Commun.*, vol. 51, no. 12, pp. 2047–2056, Dec. 2003.

[7] S. Chen, G. Dai, and W. Rao, "ICI mitigation and diversity gain for OFDM systems in time-varying multipath fading channels," *Eur. Trans. Telecommun.*, vol. 22, no. 2, pp. 61–67, 2011. [Online]. Available: http://onlinelibrary.wiley.com/doi/10.1002/ett.1458/abstract

[8] S. J. Nawaz, N. M. Khan, M. N. Patwary, and M. Moniri, "Effect of directional antenna on the doppler spectrum in 3-d mobile radio propagation environment," *IEEE Trans. Veh. Technol.*, vol. 60, no. 7, pp. 2895–2903, Sep. 2011.

[9] C. Ziółkowski and J. M. Kelner, "Antenna pattern in three-dimensional modelling of the arrival angle in simulation studies of wireless channels," *IET Microw., Antennas Propag.*, vol. 11, no. 6, pp. 898–906, 2017.

[10] O. Norklit and R. G. Vaughan, "Angular partitioning to yield equal Doppler contributions," *IEEE Trans. Veh. Technol.*, vol. 48, no. 5, pp. 1437–1442, Sep. 1999.

[11] D. Chizhik, "Slowing the time-fluctuating MIMO channel by beam forming," *IEEE Trans. Wireless Commun.*, vol. 3, no. 5, pp. 1554–1565, Sep. 2004.

[12] I. Shubhi and H. Murata, "Dynamic precoder for massive MIMO in the presence of large Doppler spread," in *Proc. IEEE 85th Veh. Technol. Conf. (VTC Spring)*, Jun. 2017, pp. 1–5.

[13] S. Serbetli and S. Baggen, "Doppler compensation by using dual antenna for mobile OFDM systems," in *Proc. IEEE Veh. Technol. Conf. (VTC-Spring)*, May 2008, pp. 1499–1503.

[14] S. Serbetli, "Doppler compensation for mobile OFDM systems with multiple receive antennas," in *Proc. IEEE 19th Symp. Commun. Veh. Technol. Benelux (SCVT)*, Nov. 2012, pp. 1–6.

[15] K. Gopala and D. Slock, "MIMO OFDM capacity maximizing beamforming for large Doppler scenarios," in *Proc. IEEE 17th Int. Workshop Signal Process. Adv. Wireless Commun. (SPAWC)*, Jul. 2016, pp. 1–6.

[16] K. Gopala and D. Slock, "High Doppler MIMO OFDM capacity maximizing spatial transceivers exploiting excess cyclic prefix," in *Proc. Int. Symp. Wireless Commun. Syst. (ISWCS)*, Sep. 2016, pp. 491–496.

[17] E. G. Larsson, O. Edfors, F. Tufvesson, and T. L. Marzetta, "Massive MIMO for next generation wireless systems," *IEEE Commun. Mag.*, vol. 52, no. 2, pp. 186–195, Feb. 2014.

[18] S. E. El-Khamy, K. H. Moussa, and A. A. El-Sherif, "C5. Performance analysis of massive MIMO multiuser transmit beamforming techniques over generalized spatial channel model," in *Proc. 32nd Nat. Radio Sci. Conf. (NRSC)*, Mar. 2015, pp. 139–146.

[19] T. L. Marzetta, "Noncooperative cellular wireless with unlimited numbers of base station antennas," *IEEE Trans. Wireless Commun.*, vol. 9, no. 11, pp. 3590–3600, Nov. 2010.

[20] F. Rusek *et al.*, "Scaling up MIMO: Opportunities and challenges with very large arrays," *IEEE Signal Process. Mag.*, vol. 30, no. 1, pp. 40–60, Jan. 2013.

[21] J. Hoydis, S. ten Brink, and M. Debbah, "Massive MIMO in the UL/DL of cellular networks: How many antennas do we need?" *IEEE J. Sel. Areas Commun.*, vol. 31, no. 2, pp. 160–171, Feb. 2013.

[22] H. Q. Ngo, E. G. Larsson, and T. L. Marzetta, "Energy and spectral efficiency of very large multiuser MIMO systems," *IEEE Trans. Commun.*, vol. 61, no. 4, pp. 1436–1449, Apr. 2013.

[23] R. H. Clarke, "A statistical theory of mobile-radio reception," *Bell Syst. Tech. J.*, vol. 47, no. 6, pp. 957–1000, Jul. 1968.

[24] W. C. Jakes, Ed., *Microwave Mobile Communications*. New York, NY, USA: IEEE Press, 1995.

[25] J. Wu and P. Fan, "A survey on high mobility wireless communications: Challenges, opportunities and solutions," *IEEE Access*, vol. 4, pp. 450–476, 2016.

[26] B. Le Floch, M. Alard, and C. Berrou, "Coded orthogonal frequency division multiplex [TV broadcasting]," *Proc. IEEE*, vol. 83, no. 6, pp. 982–996, Jun. 1995.

[27] D. Tse and P. Viswanath, *Fundamentals of Wireless Communication*. Cambridge, U.K.: Cambridge Univ. Press, 2005.

[28] Y. C. Chow, J. P. McGeehan, and A. R. Nix, "A simplified error bound analysis for M-DPSK in fading channels with diversity reception," in *Proc. IEEE GLOBECOM Commun., Commun. Theory Mini-Conf. Rec.*, Nov./Dec. 1994, pp. 13–18.

[29] H. Fu and P. Y. Kam, "Effect of Doppler shift on performance of binary DPSK over fast Rician fading channels with diversity reception," in *Proc. Int. Symp. Inf. Theory Appl.*, Dec. 2008, pp. 1–6.

[30] K. Chelli and T. Herfet, "Doppler shift compensation in vehicular communication systems," in *Proc. 2nd IEEE Int. Conf. Comput. Commun. (ICCC)*, Oct. 2016, pp. 2188–2192.

[31] R. Alieiev, T. Hehn, A. Kwoczek, and T. Kürner, "Sensor-based communication prediction for dynamic Doppler-shift compensation," in *Proc. 15th Int. Conf. Telecommun. (ITST)*, May 2017, pp. 1–7.

[32] M. Patzold, C. X. Wang, and B. O. Hogstad, "Two new sum-of-sinusoids-based methods for the efficient generation of multiple uncorrelated Rayleigh fading waveforms," *IEEE Trans. Wireless Commun.*, vol. 8, no. 6, pp. 3122–3131, Jun. 2009.

[33] *Communication System Toolbox (TM) User's Guide*. Natick, MA, USA, The MathWorks, Inc., 2016. [Online]. Available: http://www.mathworks.com/help/pdf doc/comm/

[34] *User Equipment (UE) Radio Transmission and Reception*, document TS 36.101, 3GPP. [Online]. Available: http://www.3gpp.org

[35] *Base Station (BS) Radio Transmission and Reception*, document TS 36.104, 3GPP. [Online]. Available: http://www.3gpp.org

ALEXIS BAZIN received the master's degree in telecommunications from INSA Rennes, Rennes, France, in 2015. He is currently pursuing the Ph.D. degree with Orange Labs (formerly France Telecom), Rennes. His major interests are digital communications. In particular, his applicative subjects deal with massive multiple-input multiple-output techniques and their application for the next-generation of cellular networks.

BRUNO JAHAN was born in Chinon, France, in 1966. He received the M.S. degree in optical and photonics and the M.S. degree in electronic systems from the University of Paris-Sud, Orsay, France, in 1989 and 1990, respectively. In 1991, he was with Télédiffusion de France as a Research Engineer. He joined Orange Labs (formerly France Telecom), Rennes, in 1998. His research interests include digital signals processing for wire and wireless communications.

MARYLINE HÉLARD received the M.Sc. and Ph.D. degrees from the National Institute of Applied Sciences (INSA), Rennes, in 1981 and 1984, respectively, and the Habilitation degree from the University of Rennes 1 in 2004. In 1985, she joined Orange Labs as a Research Engineer, and since 1991, she has been involved in physical-layer studies in the field of digital television and wireless communications. In 2007, she joined INSA as a Professor, where she is currently the Co-Director of the Communication Department, Institute of Electronics and Telecommunications of Rennes. In 2013, she became a Researcher with the Institut de Recherche Technologique B-Com. She was involved in several French and European collaborative research projects, including digital television, MC-CDMA, and time reversal techniques. She has co-authored of 25 patents, 30 Journal papers, and 108 conference papers. Her current research interests are in the areas of digital communications such as equalization, synchronization, iterative processing, OFDM, MC-CDMA, channel estimation, and MIMO techniques applied to wireless communications and to wire communications (ADSL, optical). She has been a General Chair of the IEEE-IWCLD 2011 and in the Steering Committee of IWCLD 2013. She has been a Guest Editor of the *IEEE Vehicular Technology Magazine* in 2014.